Journal of Organometallic Chemistry, 341 (1988) 19–38
Elsevier Sequoia S.A., Lausanne – Printed in The Netherlands

Competition among multihapto bonding, solvation, and aggregation. The η^1/η^2 infinite-chain X-ray structure of indenylsodium · *N,N,N′,N′*-tetramethyl-1,2-diaminoethane *

Christian Schade,

Institut für Chemie, Medizinische Universität zu Lübeck, Ratzeburger Allee 160, D-2400 Lübeck (Federal Republic of Germany)

Paul von Ragué Schleyer, Peter Gregory,

Institut f. Organische Chemie, Universität Erlangen-Nürnberg, Henkestr. 42, D-8520 Erlangen (Federal Republic of Germany)

Hans Dietrich, and Waruno Mahdi

Fritz-Haber Institut der Max-Planck-Gesellschaft, Faradayweg 4, D-1000 Berlin 33 (Federal Republic of Germany)

(Received September 8th, 1987)

Abstract

Indenylsodium · *N,N,N′,N′*-tetramethyl-1,2-diaminoethane (**1**; NaC_9H_7 · tmeda) crystallizes in an infinitely aggregated chain structure. Unlike the known monomeric structure of indenyllithium · tmeda, which favours η^5-coordination, the sodium cations in **1** are sandwiched between two indenyl units and, unexpectedly, exhibit η^1- and η^2-bonding. This reduction in metal coordination to each indenyl unit is due to the opportunities for interaction elsewhere, i.e. to the tmeda ligand and to a second indenyl anion. The C(1) (benzylic) sites of each indenyl unit, in turn, are coordinated in local D_{3h}-type symmetry by two metal cations on opposite faces. The structure and bonding in organosodium indenyl, fluorenyl, cyclopentadienyl, benzyl, allylenyl and allyl compounds, and in related substances, are compared. The main structure determining factors include cation radius (viz. the average cation coordination number), the charge distribution in the anion, the competition between π-delocalization due to resonance and charge localization due to the electrostatic influence of the counter-ion, hapticity, solvation and aggregation.

---

* Dedicated to Colin Eaborn on the occasion of his 65th birthday.

0022-328X/88/$03.50

Introduction

How does the nature of the counter-ion influence the structures and the electron distribution in organo-alkali metal compounds? Even though X-ray structures of organolithium compounds have been widely investigated [1*], similar determinations of organometallic compounds of the higher alkali elements are much more limited [2*]. However, the knowledge about structures of selected organosodium compounds improves our comprehension of bonding, and helps to elucidate structure determining factors in "carbanionic" compounds.

Indenylsodium · tmeda (**1**) deserves interest in relation to other compounds. Stucky and Rhine investigated the lithium analogue in 1974 [3]. Along with related structures such as diindenylmagnesium [4], counter-ion effects may be compared. From the structures of cyclopentadienylsodium · tmeda [5] or fluorenylpotassium · tmeda [6], conclusions about the role of the π-delocalized carbanions can be drawn. Finally, the largely ionic structure of **1** may be compared with the numerous transition metal indenyl complexes [7,8] and their "ring-slippage" chemistry [9].

X-Ray analysis

Crystal data. $C_{15}H_{23}N_2Na$, $M = 254.454$, orthorhombic, space group *Pbca* (D_{2h}^{15}), a 9.489(6), b 16.728(5), c 18.852(5) Å, V 2992 Å^3, $Z = 8$, D_x 1.129 g/cm^3 at 117 K. Graphite monochromated Mo-K_α radiation, λ 0.71069 Å.

Structure determination. A platelet of the dimensions $0.18 \times 0.30 \times 0.05$ mm was mounted in a glass capillary under argon. 117086 reflection profiles ($2° < \theta < 25°$) were measured at 117 K on a NONIUS CAD-4 diffractometer. Averaging yielded a unique set of 2623 structure factors, 1379 of which were stronger than 2σ. The structure was solved by direct methods (MULTAN 76 [10]) and refined on F^2 by full matrix least-squares methods (X-RAY 76 [11]) using weights $1/\sigma^2(F_0^2)$. All hydrogen atoms were introduced according to steric conditions and refined isotropically.

Two possible conformations with respect to the orientation of the CH_2CH_2 bridge in the tmeda moiety are populated 60 and 40%, respectively. The atomic positions within the bridge had therefore to be split up accordingly, while the corresponding separations of the nitrogen and methyl group positions are not big enough to be resolved, and thus remained incorporated in the "thermal" ellipsoids of these atoms. Since the separation direction of the CH_2CH_2 bridge atoms is nearly parallel to the crystallographic a^* direction, the vibration component U_{11} of these atoms had to be fixed in order to avoid correlation problems. For each pair of split positions, one value of U_{11} was chosen such that, after the refinement, the isotropic equivalents of the two tensors were approximately equal. The thermal parameters obtained in this way for the four CH_2 carbon positions were also used (after multiplication by 1.2) for the hydrogen atoms bonded to the respective carbon positions. Their positional parameters were refined and converged to approximately sensible sites.

The final R values, based on the 1379 $F_0^2 > 2\sigma$, reduced to $R(F^2) = 0.080$, $R_w(F^2) = 0.064$. The highest peak and the lowest hole in the final difference map are 0.67 and -0.77 e Å^{-3}, respectively.

* This and other references marked with an asterisk indicate notes occurring in the list of references.

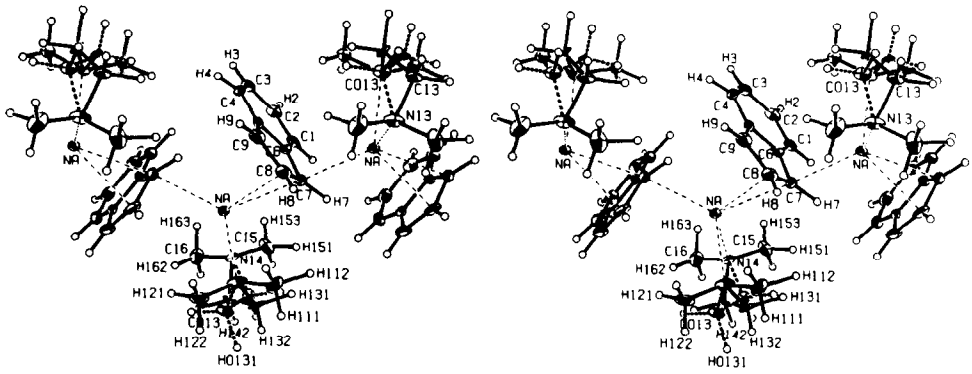

Fig. 1. Stereoscopic view (ORTEP [12]) of the crystal structure of indenylsodium·tmeda at 117 K, showing three molecular units within an infinite chain. 30% probability ellipsoids are given, except for hydrogen atoms which are represented by spheres of radius 0.1 Å. The alternative atomic positions with 40% population are connected by broken stick bonds. The numbering system is different to that used in discussing the theoretical calculations and the generalized structures.

The atomic parameters are given in Table 1. The stereoscopic view in Fig. 1 shows three molecular units within the infinite chain, to which they are linked parallel *a* by a glide plane in the crystal. In the stereoplot in Fig. 2, the tmeda group is viewed along its bonds towards sodium, in order to show more clearly the type of disorder within that part of the structure. In the parallel projection in Fig. 3, selected bond lengths and angles have been inserted.

Structure description

General. $NaC_9H_7 \cdot$ tmeda aggregates into an infinite zig-zag chain structure involving mono- and di-hapto bonding between cation and anion sites (Fig. 1). The sodium cation is close to a glide plane, which produces an infinite planar sodium chain with the angle Na″NaNa′ being 130.48(5)°, and the distance *r*(NaNa′) 5.225 Å. The tmeda groups occupy the apex positions of the chain, with the bonding plane N(13)–Na–N(14) almost perpendicular (85.2°) to the sodium plane (Fig. 2). Each indenyl group is inserted between successive sodium atoms with its plane also nearly perpendicular (89.2°) to the sodium plane. It intersects the line Na...Na′ almost in the middle, but at an angle of only 74° (cf. Fig. 1). Thus, the bonding to Na and Na′ is unsymmetrical. C(7), which is only 0.217 Å off the line Na...Na′, has a coordination of essentially D_{3h}-type local symmetry with a short bond (2.579(6) Å, Fig. 3) to Na′ and a longer one to Na, at 2.664(6) Å. C(8), which is 1.181 Å of the line Na...Na′, is only bonded to Na at 2.688(6) Å, its distance to Na′ being 3.048(6) Å. The sodium cations have a roughly capped-tetrahedral coordination, composed of two tmeda nitrogen sites, an η^1- and an η^2-bonded indenyl moiety (coordination number five).

Indenyl group. The benzene ring is essentially planar (r.m.s.d. 0.0039 Å), while the five-membered ring is slightly deformed *, presumably due to the unsymmetri-

* The planes fitted to all nine carbon atoms and to the five-membered ring yield r.m.s.d.'s of 0.0111 and 0.0101 Å.

(*Continued on p. 24*)

Table 1

Atomic parameters (e.s.d.'s in parantheses). The temperature factors are given by $T_{aniso} = \exp) - 2\pi^2(U_{11}h^2a^{*2} + U_{22}k^2b^{*2} + U_{33}l^2c^{*2} + 2U_{12}hka^*b^* + 2U_{13}hla^*c^* + 2U_{23}klb^*c^*))$; $T_{iso} = \exp(-2\pi^2 \cdot 2U \sin(\theta)^2/\lambda^2)$

Atom	Population	x	y	z	$U11$ or U	$U22$	$U33$	$U12$	$U13$	$U23$
Na		0.1755(2)	0.6907(1)	0.80804(8)	0.024(1)	0.022(1)	0.0162(9)	−0.001(1)	−0.0010(9)	0.0002(9)
C(1)		0.4159(6)	0.5267(4)	0.7380(3)	0.031(4)	0.051(4)	0.022(3)	0.015(3)	0.006(3)	0.000(3)
C(2)		0.3496(6)	0.4684(4)	0.6991(3)	0.051(5)	0.037(4)	0.036(4)	0.008(4)	0.013(3)	−0.003(3)
C(3)		0.2552(7)	0.4886(4)	0.6443(3)	0.039(4)	0.054(4)	0.031(3)	−0.008(4)	0.010(3)	−0.014(3)
C(4)		0.2248(6)	0.5665(4)	0.6286(3)	0.024(4)	0.079(5)	0.016(3)	−0.002(4)	−0.003(3)	−0.005(3)
C(5)		0.2892(5)	0.6288(3)	0.6678(2)	0.017(3)	0.048(4)	0.018(3)	0.001(3)	0.003(2)	0.005(3)
C(6)		0.3867(5)	0.6076(3)	0.7236(2)	0.024(3)	0.04494)	0.013(3)	0.004(3)	−0.003(2)	−0.005(3)
C(7)		0.4348(6)	0.6798(4)	0.7547(3)	0.022(3)	0.059(4)	0.019(3)	−0.006(4)	−0.000(2)	0.004(3)
C(8)		0.3723(6)	0.7438(4)	0.7169(3)	0.045(4)	0.048(4)	0.025(3)	−0.013(3)	0.014(3)	0.005(3)
C(9)		0.2838(7)	0.7126(3)	0.6645(3)	0.045(4)	0.046(4)	0.023(3)	0.002(3)	0.008(3)	0.013(3)
C(11)		0.3438(7)	0.8513(4)	0.8787(4)	0.041(5)	0.048(4)	0.069(5)	−0.011(4)	−0.015(4)	−0.026(4)
C(12)		0.0969(8)	0.8517(5)	0.9032(4)	0.061(6)	0.060(5)	0.044(5)	−0.023(5)	0.014(4)	−0.033(4)
N(13)		0.2200(6)	0.8021(2)	0.8956(2)	0.075(4)	0.017(2)	0.024(2)	−0.004(3)	−0.008(3)	−0.003(2)
C(13)	0.60	0.287(1)	0.7583(7)	0.9579(5)	0.0500	0.035(7)	0.010(5)	−0.016(7)	−0.012(6)	−0.004(5)
C(14)	0.60	0.195(1)	0.687(1)	0.9800(7)	0.0300	0.027(7)	0.016(5)	−0.010(9)	0.020(6)	−0.008(5)
N(14)		0.2021(5)	0.6250(2)	0.9232(2)	0.033(3)	0.016(2)	0.016(2)	−0.002(2)	−0.008(2)	−0.000(2)
C(15)		0.3259(8)	0.5742(5)	0.9213(3)	0.042(4)	0.076(5)	0.024(3)	0.029(5)	0.006(4)	0.019(4)
C(16)		0.0785(7)	0.5778(5)	0.9413(3)	0.037(4)	0.066(6)	0.032(4)	−0.004(4)	−0.003(3)	0.018(4)
C(013)	0.40	0.181(2)	0.7622(9)	0.9677(7)	0.0500	0.023(8)	0.024(7)	0.02(1)	0.00(1)	−0.003(7)
C(014)	0.40	0.262(2)	0.688(2)	0.970(1)	0.0300	0.03(1)	0.015(9)	−0.01(1)	0.00(1)	0.017(8)

H(1)		0.488(5)	0.514(3)	0.776(2)	0.06(2)					
H(2)		0.369(5)	0.412(3)	0.705(2)	0.06(2)					
H(3)		0.201(5)	0.447(3)	0.618(2)	0.06(2)					
H(4)		0.151(5)	0.580(3)	0.598(2)	0.03(1)					
H(7)		0.522(6)	0.687(4)	0.787(2)	0.09(2)					
H(8)		0.401(4)	0.801(3)	0.727(2)	0.04(2)					
H(9)		0.227(5)	0.740(3)	0.633(2)	0.05(2)					
H(111)		0.364(5)	0.885(3)	0.921(2)	0.06(2)					
H(112)		0.460(8)	0.822(5)	0.870(3)	0.17(3)					
H(113)		0.312(7)	0.885(3)	0.835(2)	0.10(2)					
H(121)		0.006(6)	0.820(3)	0.908(2)	0.06(2)					
H(122)		0.100(5)	0.885(3)	0.947(2)	0.06(2)					
H(123)		0.077(5)	0.883(3)	0.863(2)	0.03(2)					
H(131)	0.60	0.407(9)	0.740(5)	0.945(4)	0.0600	0.0419	0.0123	−0.0197	−0.0143	−0.0051
H(132)	0.60	0.302(9)	0.782(5)	0.994(4)	0.0600	0.0419	0.0123	−0.0197	−0.0143	−0.0051
H(141)	0.60	0.09(1)	0.697(5)	0.991(3)	0.0360	0.0323	0.0187	−0.0125	0.0235	−0.0091
H(142)	0.60	0.212(8)	0.654(4)	1.037(3)	0.0360	0.0323	0.0187	−0.0125	0.0235	−0.0091
H(151)		0.429(5)	0.607(3)	0.909(2)	0.07(2)					
H(152)		0.346(4)	0.553(2)	0.968(2)	0.03(1)					
H(153)		0.317(6)	0.535(3)	0.888(2)	0.07(2)					
H(161)		0.089(5)	0.552(3)	0.989(3)	0.07(2)					
H(162)		0.003(6)	0.617(3)	0.943(2)	0.05(2)					
H(163)		0.077(5)	0.530(3)	0.901(2)	0.06(2)					
H(0131)	0.40	0.22(1)	0.810(6)	1.016(5)	0.0600	0.0275	0.0293	0.0205	0.0039	−0.0040
H(0132)	0.40	0.07(1)	0.751(9)	0.974(6)	0.0600	0.0275	0.0293	0.0205	0.0039	−0.0040
H(0141)	0.40	0.29(1)	0.672(6)	1.018(5)	0.0360	0.0322	0.0179	−0.0125	0.0027	0.0201
H(0142)	0.40	0.37(1)	0.693(8)	0.961(5)	0.0360	0.0322	0.0179	−0.0125	0.0027	0.0201

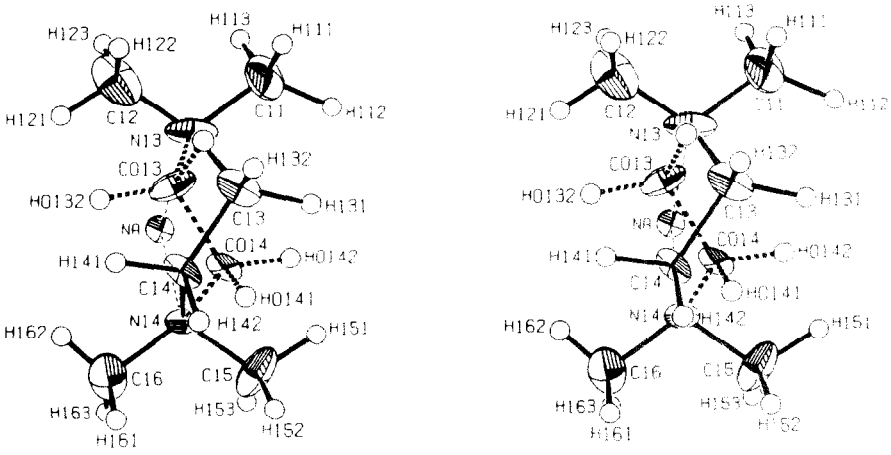

Fig. 2. Stereoscopic plot (ORTEP [12]) of the tmeda group viewed towards its convex side at 117 K. 50% probability ellipsoids are given, except for hydrogen atoms which are represented by spheres of radius 0.1 Å. The alternative positions with 40% population are connected by broken sticks.

cal bonding to the cations. The deformations can best be described by the deviations from the plane fitted to the benzene ring. While C(7) is shifted 0.02 Å towards Na, C(8) and C(9) are shifted 0.02 and 0.03 Å respectively towards Na′. Less accurate are the shifts of H(7), 0.20 Å, and H(8), 0.12 Å, towards Na′.

The tmeda group. The tmeda group is severely disordered (Fig. 2). The end carrying the methyl groups C(16) and C(15) is embedded between benzene rings, whereas the five-membered rings leave a little more space for the other end carrying the methyl groups C(11) and C(12) (cf. Fig. 1). This is probably the reason for the large separation of 1.03(3) Å of the alternative methylene positions C(13) and C(013), compared with 0.66 Å in case of C(14) and C(014).

The two conformers of the tmeda group fit into the available space without causing short contacts to neighbouring ligands. The indenyl atoms C(9)*–H(9)* approach the convex side of the tmeda group, with H(9)* pointing into the central gap between the methylene hydrogen positions H(132), H(0131), H(142), and H(0141). Moreover, from a model of the structure, it can be seen that C(9)*–H(9)* should not even hinder the transition between the two alternative conformers of the tmeda group.

Since the X-ray structure is averaged over time and crystal volume, a distinction between a static (frozen) and a dynamic disorder (possibly coupled with lattice vibrations) cannot be given. The fact that all hydrogen positions could be refined is no proof for a static disorder because the time needed for the transitions between the conformers is presumably short compared with the half life of the conformers, at least at low temperature. One condition for the fact that both conformers fit into the available space is a considerable mobility of the nitrogen atoms around the surface of the sodium atom. This mobility is evident from the large anisotropy of the N ellipsoids in Fig. 2. This is in contrast to most tmeda · Li organic structures, in which the Li–N bonds seem to be much more rigid and usually are not involved in the conformational disorder (see below).

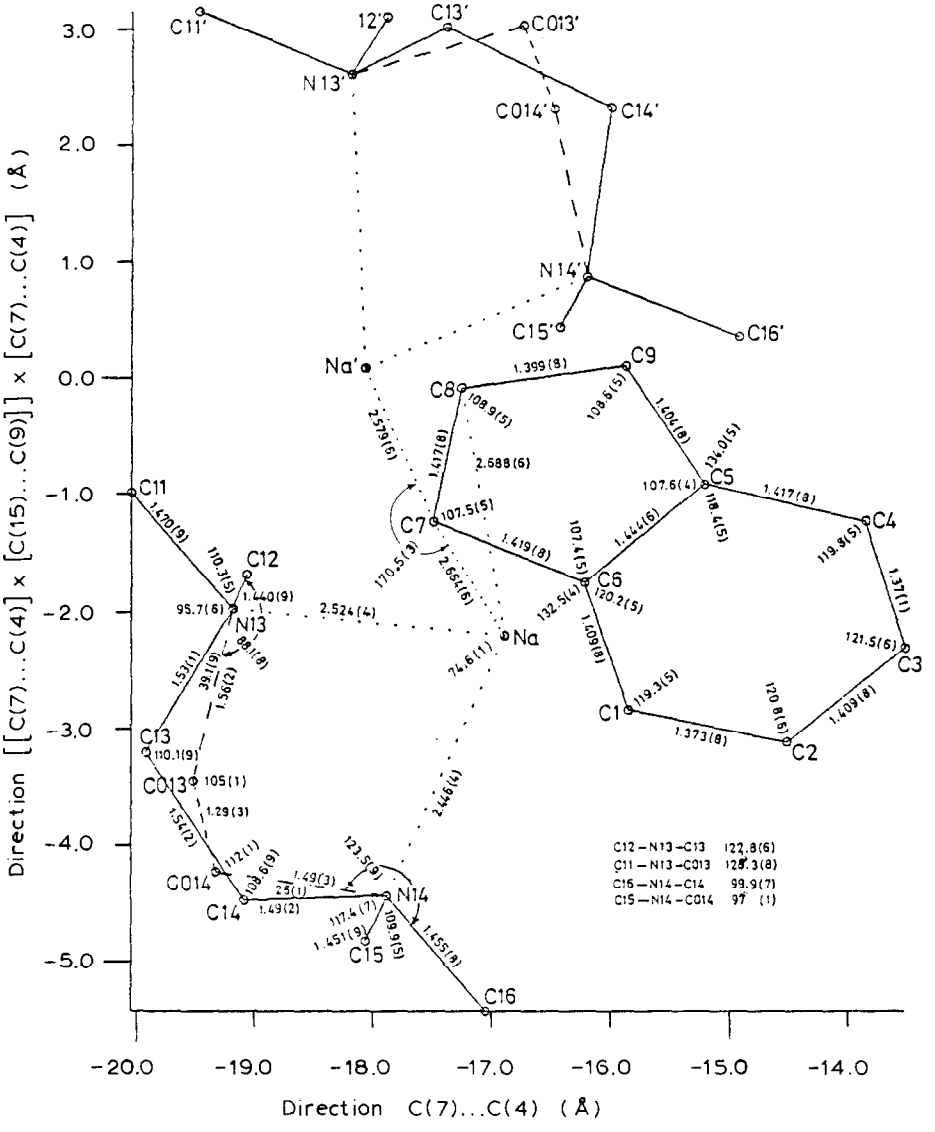

Fig. 3. Projection of the indenyl group, and the two tmeda-Na groups bonded to it. Hydrogen atoms are omitted for clarity; selected bond lengths and angles are included (e.s.d.'s in parentheses). The alternative positions with 40% population are connected by broken lines. The numbering system is different to that used in discussing the theoretical calculation and the generalized structures.

Discussion

Structure determining factors. How can the structure of **1** be deduced from general bonding considerations [2]? We first outline the main structure determining factors and then develop our model by further comparisons with related systems.

The average coordination number of the alkali ion in essence is determined by the cation radius. For sodium, five is the most commonly chosen organometallic

coordination number [2], as in **1**. Anion, ligand and neighbouring anion (aggregation) sites compete for the coordination available. The observed structure corresponds to the most favourable of all these nucleophile–electrophile interactions. In most cases, the cation–anion interaction is the most important. Since alkali metal bonding is largely ionic [13], the alkali cations interact with the carbon centres with the highest charge density. As given by Hückel MO [14] and by MNDO [15] calculations, the highest charge density in the indenyl anion is at the benzyl-type positions, C(1) and C(3); the main interaction of the sodium cations in **1** is with one of these symmetry-related sites. A close approach of a cation to a single site polarizes the anionic charge distribution due to coulombic interaction. For π-delocalized carbanions, this "charge localization" mechanism [16] restricts the cation–anion interaction to one or two coordination sites in many organoalkali compounds [1,2]. However, the "charge localization" competes with π-delocalization, which favours multihapto coordination and a more symmetrical placement of the counter-ion. The major energy term determines the result: for highly symmetrical systems with the largest π-delocalization energies (e.g. the aromatic cyclopentadienyl anion), multihapto bonded structures are favoured, whereas in systems of lower symmetry where localization of charge is easier (e.g. the benzyl anions), coordination restricted to fewer sites is the rule. Partial charge localization at C(1) of the indenyl anion is not very expensive energetically, and the π-resonance energy in the benzene part and the allyl anion moiety of the molecule remains intact.

Additional anion sites (multihapto bonding), solvent molecules (ligand), and aggregation (i.e. a second anion as a moderated ligand) compete with one another for the remaining coordination available at the metal centre. Since alkali cation solvation energies by neutral nitrogen nucleophiles are generally larger than those by neutral carbon nucleophiles [17] *, tmeda chelation is preferentially included into the sodium coordination sphere of **1**. The halfway placement C(7)..Na..C(7′) and the short distances r(NaC) 2.6 Å demonstrate strong aggregation among the ion pairs. These interactions still leave one coordination site available at the sodium centre. Additional aggregation or solvation would probably induce steric crowding, and the coordination sphere is completed by moderate increase in hapticity (η^2-bridging of C(7′) and C(8′)) instead.

The η^1/η^2-attachment of the sodium cation to the indenyl moiety is unexpected, and not in line with related structures such as indenyllithium · tmeda [3] and cyclopentadienylsodium · tmeda [5] (see below). We therefore wish to describe factors determining the hapticity of alkali cations. Qualitatively, the haptotropic search [18] of the metal cation is controlled by charge localization, π-delocalization, aggregation, and solvation. Solvation and aggregation are favoured over multihapto bonding, if their interaction energies are larger than the energy differences for the different haptomers. The ion-pair structure in turn aggregates into clusters or chains, if both ligand and multihapto interaction do not effectively coordinate the metal cation. Estimates of the magnitude of these contributions can be obtained via appropriate model calculations.

Hapticity; MNDO calculations. Potential energy surfaces for metal cations located above a delocalized anion often are quite flat [19,20]. Energy differences

* Here we consider the indenyl anionic charge as localized at the C(7) position, and compare the sodium interaction with the π-system C(1)...C(6),C(8),C(9) vs. that with other "ligands".

Table 2

Relative energies (kJ mol^{-1}) of indenyl species

Haptomer	Point charge model [14]	Indenyllithium, MNDO
η^5	0.0	0.0
η^6	50.6[a]	15.9
η^1	61.5[a]	48.1[a]
η^2		64.0[a]
$\eta^5 \cdot OH_2$		0.0
$\eta^6 \cdot OH_2$		13.8
$\eta^1 \cdot OH_2$		45.6[a]
$\eta^2 \cdot OH_2$		59.0[a]
$\eta^5 \cdot (OH_2)_2$		0.0
$\eta^6 \cdot (OH_2)_2$		11.3
$\eta^1 \cdot (OH_2)_2$		33.5[a]
$\eta^2 \cdot (OH_2)_2$		40.6[a]
$\eta^5 \cdot (OH_2)_3$		0.0
$\eta^6 \cdot (OH_2)_3$		12.1
$\eta^1 \cdot (OH_2)_3$		18.0[a]
$\eta^2 \cdot (OH_2)_3$		33.5[a]
$\eta^5 \cdot (OH_2)_4$		0.0
$\eta^6 \cdot (OH_2)_4$		18.8
$\eta^1 \cdot (OH_2)_4$		5.9[a]
$\eta^2 \cdot (OH_2)_4$		19.7[a]

[a] The structures are not minimal. They have been calculated by fixing the metal cation or the point charge over the ring or in the position indicated.

among isomers of different hapticity generally decrease with increasing cation–anion distance, and with increasing numbers of ligands bound to the cation.

Electrostatic calculations for a point charge above the indenyl anion give a single minimum with the point charge located in the η^5-position to the five-membered ring [20]. However, further minima are created when additional point charges (ligands) are included outside to the indenyl system [20b]. The η^5-haptomer is the global minimum for indenyllithium $\cdot (H_2O)_x$ ($0 \leq x \leq 4$) by MNDO calculations [15]. In the unsolvated system, the η^6-haptomer is a second minimum, relatively destabilized by 15.9 kJ mol^{-1}. The η^1 and η^2 haptomers are not minima, and are 48.1 and 64.0 kJ mol^{-1} higher in energy. However, as the lithium cation is progressively solvated with water, these become relatively stabilised. With additional solvent molecules, the distance of closest cation–anion approach increases and the energy difference between the haptomers is reduced, favouring the haptomers with lower coordination to the anion (see Tables 2 and 3). For all systems, the average lithium–carbon distance increases with increasing hapticity.

On solvation in the η^5-haptomer, the lithium cation moves gradually away from C(8) and C(9) towards C(2), in an attempt to redress the hapticity balance. With three or four water ligands, the distances between the cation and C(8) and C(9) increase dramatically, resulting in a pseudo η^3-haptomer. This reduction in coordination agrees with the observed structure of indenyllithium in solution [3], and parallels the transition metal ring-slippage chemistry [9]. In an analogous manner, the lithium cation moves away from the central position above the six-membered ring towards C(5) and C(6) when the η^6-haptomer is progressively solvated. The figures for the η^1-haptomer demonstrate the increase in the cation–anion distance caused by the stepwise solvation. The increase in the C(1)–C(2) and C(1)–C(8) bond

Table 3

MNDO bond lengths (in Å) for indenyllithium·$(H_2O)_x$ haptomers

Haptomer	Li–C(1,3)	Li–C(2)	Li–C(8,9)
η^5	2.176	2.182	2.227
η^5·(OH_2)	2.203	2.202	2.252
η^5·$(OH_2)_2$	2.271	2.256	2.310
η^5·$(OH_2)_3$	2.332	2.302	2.427
η^5·$(OH_2)_4$	2.419	2.337	2.585
Haptomer	Li–C(8,9)	Li–C(4,7)	Li–C(5,6)
η^6	2.241	2.276	2.236
η^6·(OH_2)	2.271	2.295	2.257
η^6·$(OH_2)_2$	2.340	2.371	2.317
η^6·$(OH_2)_3$	2.440	2.431	2.390
η^6·$(OH_2)_4$	2.584	2.530	2.446
Haptomer	Li–C(1)		
η^1	1.957		
η^1·(OH_2)	1.986		
η^1·$(OH_2)_2$	2.027		
η^1·$(OH_2)_3$	2.097		
η^1·$(OH_2)_4$	2.155		
Haptomer	Li–C(1,8)		
η^2	2.054		
η^2·(OH_2)	2.102		
η^2·$(OH_2)_2$	2.149		
η^2·$(OH_2)_3$	2.235		
η^2·$(OH_2)_4$	2.322		

lengths relative to those in the η^5- and η^6-haptomers by ca. 0.04 Å indicates the partial localization of charge in the η^1 haptomer.

The case with four solvating water molecules probably reflects over-solvation of the lithium cation, resulting in a somewhat unrealistic relative destabilisation of the η^5-, and especially the η^6-haptomer. This would be less of a problem with the larger sodium cation.

The π-charges calculated for the free anion correlate better with the observed ^{13}C NMR shifts than those calculated for the solvated ion pairs. This would imply that indenyllithium exists as solvent-separated ion pairs in THF solution [21]. The slope of the least-squares function for the free anion has the value 161.7 ($r = 0.980$), which agrees well with the value of 156.3 ppm/unit charge predicted by O'Brien [22].

Direct observation of equilibrating η^6-η^5-(fluorenyl)$Cr(CO)_2L$ anions yielded a net stabilization of 8–10 kJ mol^{-1} of the η^6- vs. the η^5-species [23]. However, with increasing electron-withdrawing ability of the chromium moiety, the η^5-haptomer becomes relatively stabilized.

Related structures. The homologous ion sequence. Indenyllithium · tmeda, (**2**) [3] crystallizes as an ion pair with η^5-attachment of the lithium cation to the indenyl anion. Since the larger sodium cation requires further coordination, **1** aggregates into an infinite chain with simultaneous reduction of hapticity. Analogously cyclopentadienyllithium compounds exhibit ion-pair structures [24], whereas NaC_5H_5 ·

tmeda (**3**) forms an aggregated chain structure [5], similar to **1**. However, as the large aromatization energy and D_{5h} symmetry of the cyclopentadienyl anion cannot be overcome by the charge localizing influence of the metal cation, the η^5-interaction is maintained in the crystal structure of **3**. There is a dilemma for **3**, since an ion-pair structure would not complete the sodium coordination, and the aggregated chain structure induces an unusually large sodium coordination sphere. **1** evades this dilemma by charge localization at the indenyl-C(1) position. The shortest distance r(NaC) in **1**, 2.58 Å, is as short as r(NaC) in CH_3Na [25], while the average distance r(NaC) 2.92 Å in **3** is among the larger distances reported [2]. In the more restricted coordination sphere of ethanoylcyclopentadienylsodium · THF [26] (one η^5-cyclopentadienyl unit, three oxygen sites), the average distance r(NaC) decreases to 2.83 Å. Similarly, in $Na(THF)_3[Sb_4(C_5H_3)_4(C_5H_5)]$, three THF molecules coordinate to the sodium cation which is bonded η^5 to a cyclopentadienyl unit at r(NaC) 2.70–2.84 Å (2.78 Å av.) [27]. $K(C_5H_4SiMe_3)$ [28] forms a puckered chain structure like **3**. The distance r(KC) 3.03 Å is only 0.12 Å larger than r(NaC) in **3**, even though the average ion radius difference is Δr 0.4 Å for both cations. Cyclopentadienyl rings are bis-η^5-coordinated to the metal in $Mg(C_5H_5)_2$ [20]. By analogy to **3**, this type of coordination is retained in the puckered Lewis base adducts $Mg(C_5H_5)_2 \cdot L_2$, with probable increase of Mg–C_5H_5 distances [30]. However, in $Be(C_5H_5)_2$ (η^1,η^5) [31] and $Ca(C_5H_5)_2$ (η^5,η^5,η^4,η^1) [32], restricted hapticities have been observed.

Dilithionaphthalene · $(tmeda)_2$ [33] crystallizes as an ion-pair; the lithium cations are η^6-associated with the aromatic ring faces. In contrast, 1,8-dimethylnaphthylsodium · tmeda [34] is ring-metallated and forms an infinite zig-zag puckered chain structure with the sodium cations bis-η^2-coordinated to the organic group.

Fluorenyllithium · bisquinuclidine (**4**) [35] forms an ion-pair structure with charge localization at C(9) and C(1). The larger cation in fluorenylpotassium · tmeda expands the charge localized coordination in **4** to multihapto bonding, residing at an η^5-coordinated site above two anion planes [6], forming a puckered chain in close analogy to **1** and **3**.

In conclusion, we elucidate a sequence for organoalkali compounds with π-delocalizable anions: ion pair with restricted cation–anion interaction, ion pair with multihapto anion coordination, aggregated chain with restricted interaction, aggregated chain with multihapto interaction, higher aggregated species. Depending on the available coordination sites at the metal centre (i.e. the cation radius and presence of additional ligands), one of these structure types will be chosen. The homologous cation, due to its increase in ion size, adopts the next structure within the sequence in general. Inclusion of additional solvent sites favours the reverse step (Table 4) [36*].

Such considerations predict indenyllithium · pmdta (pmdta = 1,1,4,7,7-pentamethyl-1,4,7-triazaheptane) to be an η^1-bonded ion pair, while indenylsodium · pmdta should be analogous to indenyllithium · tmeda. Experimental evidence arises for indenylsodium, since the aggregates are believed to dissociate into ion pairs with η^5-bonding of the cation to the anion in pyridine solution [21c]. Similar findings have been made in other solvents [21].

The zig-zag puckered chain. Zig-zag puckered chain structures are not only very common among alkali cyclopentadienyl [5,28], indenyl, fluorenyl [35], benzyl [37,38] (see below), and naphthyl [34] compounds. In isolobal analogy, $Tl(C_5H_5)$ [39],

Table 4

Hapticity of selected organoalkali solid state structures

Restricted ion pair	Multihapto ion pair	Restricted aggregate	Multihapto ion pair
	$Me_3SiC_5H_4Li \cdot$ tmeda (η^5) [24a]		$C_5H_5Na \cdot$ tmeda (η^5) [5]
			$Me_3SiC_5H_4K$ (η^5) [28]
	indenyllithium · tmeda (η^5) [3]	indenylsodium · tmeda (η^1, η^2)	
----fluorenyllithium · bisquinuclidine (η^3) [35]----			
			Fluorenylpotassium · tmeda (η^5) [6]
----benzyllithium · dabco [a] (η^3) [71]----		benzylsodium · tmeda (η^1,(η^2)) [38]	
		benzyllithium · Et_2O (η^1,(η^2)) [37]	
	dilithionaphthalene · $(tmeda)_2$ (η^6) [33]	1,8-diphenylnaphthylsodium · tmeda (η^2) [34]	

[a] dabco = 1,4-diazabicyclo[2.2.2]octane.

$In(C_5H_5)$ [40], $Pb(C_5H_5)_2$ [41], $Tl(C_5Me_5)$ [42], $Tl\{C_5H_4C_2(CN)_3\}$ [43], and $ZnMe(C_5H_5)$ [44] adopt a structure related to that of **3** with Tl^+, In^+, $Pb(C_5H_5)^+$, and $ZnMe^+$ replacing the Na(tmeda) + fragment, respectively. Restricted η^1-attachment of the metal to the cyclopentadienyl unit is found in the chain structures of $Me_2Al(\mu\text{-}\eta^1 : \eta^1\text{-}C_5H_5)$ [45], $(\eta^5\text{-}C_5H_5)_2Sc(\mu\text{-}\eta^1 : \eta^1\text{-}C_5H_5)$ [46], and $(\eta^5\text{-}C_5H_5)_2La(\mu\text{-}\eta^2 : \eta^5\text{-}C_5H_5)$ [47].

Finally, the transition metals are capable of forming related chain structures, e.g. the low temperature modification of $(C_5H_5)Mn(\mu\text{-}\eta^1 : \eta^1\text{-}C_5H_5)$ [48] and $Ni(\mu\text{-}\eta^5 : \eta^5\text{-}Me_4C_3B_2)$ [49].

η^1-Bonding. η^1-Bonding in largely ionic indenyl compounds has been found in diindenylmagnesium [4]. Each metal centre is η^5-coordinated to one indenyl moiety. These $C_9H_7Mg^+$ fragments are isolobal to sodium cations and build up a chain structure related to **1** with η^1- and η^2-coordination to the remaining indenyl units. Samarium in $Sm(C_9H_7)_3$ [7c] is η^5-coordinated to the indenyl ring systems, with no evidence for η^1-type coordination: in THF solution, NMR results indicate monohapto bonding [50a,b].

From the disconnection of the indenyl anion into a benzene and an allylic part, another analogy to **1** emerges, since lithium cations in allyllithium coordinate either η^1 [51] or η^2 [52] to the allylic moiety. In 1,3-diphenylallyllithium · Et_2O [53], probably due to the increase in resonance energy of the organic moiety, the lithium cation resides in the η^3-position.

Transition metals usually are bound η^5 [7] or η^3 [8] to the indenyl unit. However, there is spectroscopic evidence that η^1-attachment of the metal to the C(1) position is feasible as well [7x,50]. Thus, in addition to the rare η^6-bonding via the benzene subunit [7ab,54], three different bonding sites are readily available at the indenyl C_5 moiety. The existence of the related ionic compounds **1** and **2** in the very different η^1/η^2- and η^5-coordinations suggests that energetic differences between the haptomers are small in solution, where solvent molecules can easily replace vacant coordination sites. The structures of **1** and **2** further support the "indenyl effect" hypothesis [55], i.e. the lability of indenyl compounds in comparison to cyclopentadienyl analogues [9]. Dearomatization of the cyclopentadienyl system in η^3, or η^1-haptomers is more costly, and cyclopentadienylalkali compounds generally remain η^5-coordinated. The chemistry of transition metal complexes finds analogies among organoalkali structures.

The transition states of fluxional η^1-cyclopentadienyl compounds probably involve η^2-bonding to the hydrocarbon similar to that in **1** [56].

The indenyl unit. Since bond distances within the hydrocarbon moiety do not vary much in indenylmetal compounds, it is justified to average published data (Fig. 4, [7]) *. In general, bond lengths within the six-membered ring are shorter than those of the five-membered ring (1.400 Å vs. 1.423 Å). This strongly suggests enhanced electron density within the five-membered ring, as predicted by calculations for the free anion. The indenyl moiety thus represents a benzannelated cyclopentadienyl structure. Variations in bond lengths within the benzene moiety follow a consistent pattern: C(4)–C(5) and C(6)–C(7) are shorter, while C(4)–C(9), C(5)–C(6) and C(7)–C(8) are slightly longer. The difference is ca. 0.04 Å between

* η^3-Bonded compounds with considerable folding of the five-membered ring [8] have been excluded, since they show large deviations for the five-membered ring parameters.

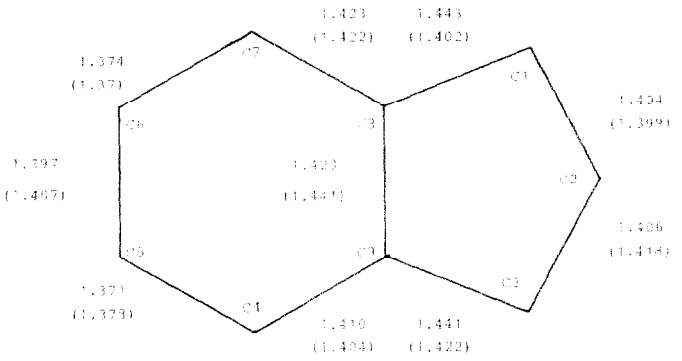

Fig. 4. Averaged carbon–carbon bond lengths (in Å) of indenylmetal compounds from ref. 7: data for **1** are given in parentheses. The numbering system is different to that used in the structural determination of indenylsodium · tmeda.

these sets, as in **1**. These numbers are reproduced by the MNDO calculations on indenyllithium · $(H_2O)_x$. Cyclopentadienyl annelation favors a greater contribution by one of the resonance structures of the benzene subunit [7b,7h,7j], but the transannular bond C(8)–C(9) is quite long (1.441 Å in **1**).

Bond lengths within the cyclopentadienyl unit vary considerably for different compounds with no clear cut correlation with any one resonance contributor. Due to the η^1/η^2-bonding mode of the sodium cation in **1**, bonds connecting the metal binding site C(1) are lengthened, reflecting the partial localization of the anion charge.

The C–C distances in indenyllithium · tmeda **2** agree reasonably well with those in **1**, even though the symmetric η^5-position of the lithium cation produces a more regular bond length pattern within the five-membered ring [3]. Due to the symmetric placement of both cations, the C_9H_7 ring is fairly planar in **1**, while C(1) and C(3) are slightly displaced towards the lithium cation in **2**.

The tmeda ligand. Formation of tmeda chelates is very common for organolithium compounds. Entropy, rather than enthalpy, provides the driving force for the coordination of the lithium cation by the bidentate ligand. From model calculations [57], tmeda chelation of Li^+ is endothermic compared to the solvation by two independent amine molecules, but the entropy term is less unfavourable for tmeda. An analysis of Li^+/tmeda chelates suggests non-optimal interaction between the metal cation and the ligand, since the average angle N–Li–N′ 84° is considerably smaller than tetrahedral. Nevertheless, Stucky derived the best lone-pair orientation in tmeda chelates for N–metal–N′ = 85°, i.e. for lithium cations [6].

Table 5 contains a survey of the steric aspects of some tmeda chelates. The angles M–E–N (= metal–N lone pair–N) show that the lone pairs do not point towards the metal. The angles E–M–E are always greater than N–M–N, i.e. the chelate bonds M–N are actually bent bonds with the lone pairs essentially within the plane N–M–N but outside the triangle N–M–N. The bending of the chelate bonds probably causes a strain on the angles N–C–C, which appear to be slightly widened to about 112°. The widening of these angles should, on the other hand, lower the energy barrier between the two conformers of the tmeda group. In the case of the tmeda · Li chelates, the angles E–Li–E are not too far from tetrahedral, which

Table 5

Steric analysis of some tmeda chelates of lithium and sodium. Two lines per tmeda, starting with the angles N–C–C, followed by the angles M–E–N, where E is the lone pair position at N. E is assumed to be shifted 0.5 Å from the N position perpendicular to a plane defined by unit vectors along the three N–C bonds. Angles in degrees, e.s.d.'s in parentheses; for the (weighted) average values the r.m.s.d.'s are given instead

	Angles				
	N–C–C	M–E–N	E–M–E	N–M–N′	Ref.
$(PhCH)_2CO\cdot\{Li(tmeda)\}_2$	111.1(1)	170.5(1)	100.7(2)	87.92(8)	58
	111.4(1)	158.8(1)			
$PhCHCCCHPh\cdot\{Li(tmeda)\}_2$	111.0(2)	168.0(2)	98.1(4)	86.7(2)	1, 59
	111.5(3)	166.6(3)			
$PhCHC_9H_6\cdot\{Li(tmeda)\}_2$	111.18(9)	163.1(1)	99.5(2)	87.51(8)	1, 59
	111.3(1)	161.0(1)			
	112.0(1)	158.2(1)	102.4(2)	88.17(8)	
	111.691)	162.7(1)			
$(PhCH)_2C_6H_4\cdot\{Li(tmeda)\}_2$	117.(1)	171.(1)	96.(2)	87.1(6)	60
	120.(1)	170.(1)			
	116.(1)	164.(1)	102.(2)	89.5(6)	
	117.(1)	165.(1)			
$Ph(CH_4Ph\cdot\{Li(tmeda)\}_2$	111.0(2)	163.4(2)	99.8(3)	86.6(2)	61
	111.4(2)	158.8(2)			
$(C_6H_4)_2O\cdot\{Li(tmeda)\}_2$	112.05(6)	158.06(6)	96.9(1)	85.10(5)	1, 62
	112.10(6)	158.06(6)			
	110.87(6)	168.72(6)	97.1(1)	86.95(5)	
	111.74(6)	160.09(6)			
$\{PhC_6H_4\cdot Li(tmeda)\}_2$	113.6(4)	165.7(4)	89.8(6)	80.2(2)	1, 62
	112.3(3)	167.0(3)			
$Ph_4C_4\cdot\{Li(tmeda)\}_2$	111.1(5)	159.9(5)	91.9(7)	84.2(3)	1, 59
	111.3(5)	175.4(5)			
C_5H_4-$SiMe_3Li\cdot tmeda$				84.9	24a
$C_9H_7Li\cdot tmeda$				86.4	3
$\{PhLi\cdot tmeda\}_2$				84.3	63
$Ph_3CLi\cdot tmeda$				88.5	64
$(PhCHCHPh)\cdot\{Li(tmeda)\}_2$				86.1	65
Li·tmeda average (r.m.s.d.'s)	111.6(5)	163.(4)	98.(2)	86.(2)	
1	110.1(9)	167.9(9)	80.(1)	74.6(1)	this work
	108.6(9)	176.7(9)			
$\{PhCH_2Na\cdot tmeda\}_4$	113.(1)	172.(1)	79.(2)	74.3(1)	38
	111.(1)	174.(1)			
	113.2(9)	167.7(9)	80.(1)	74.5(1)	
	113.(1)	175.(1)			
	111.(1)	175.(1)	79.(2)	74.5(1)	
	113.(1)	170.(1)			
	110.(1)	173.(1)	75.(2)	72.9(1)	
	112.(1)	171.(1)			
$C_5H_5Na\cdot tmeda$				70.5	5
$Ph_3CNa\cdot tmeda$				76.6	66
$Me_3CC{=}CC(Me)C{=}C{=}CCMe_3Na$					
$\cdot(tmeda)_2$				70.3	67
				71.2	
$\{Ni_2H(C_2H_4)_4\}Na\cdot(tmeda)_2$				74.9	68
				73.7	
$\{C_{10}H_9Na\cdot tmeda\}_2$				72.5(2)	34
$Ph_4LiNa_3\cdot(tmeda)_3$				72.8(3)	34
				72.3(3)	
				71.4(2)	

Table 5 (continued)

	Angles				
	N–C–C	M–E–N	E–M–E	N–M–N′	Ref.
$\{2\text{-}CH_3C_6H_4CH_2Na \cdot tmeda\}_4$				74.6(2) 73.7(2)	34
$\{(4\text{-}CH_3C_6H_4CH_2)(NMe_2)_5Na_6 \cdot (tmeda)_2\}_2$				72.2(5)	34
Na–tmeda average (r.m.s.d.'s)	112.(2)	172(3)	79.(2)	73.(2)	
$C_{13}H_9K \cdot tmeda$		bridging ligand		90.4	6

explains the observed rigidity of the N–Li–N chelate bond system.

For cations of greater size, the bonding situation becomes worse, as the cation slips out of the "bite" of the tmeda ligand. The average angle N–Na–N reduces to ca. 74° (Table 5). Since solvation energies decrease with increasing ion size, the enthalpy difference between a chelated system and that solvated by two independent ligands will not increase as much as expected from the inferior bite of the tmeda chelate alone, and Na(tmeda)$^+$ chelates are still favoured due to entropy. The price to be paid is seen from the crystal structures, since disorder of the ligand methylene bridge is more severe in sodium than in lithium compounds. The less satisfactory chelation, and the weaker Na–N interaction energies, permit larger conformational flexibility of the five-membered Na(tmeda)$^+$ ring structures. For **1**, even the coordinating nitrogen sites are subject to structural disorder (see above).

Finally, in fluorenylpotassium · tmeda [6], the ligand is no longer able to chelate the potassium ion efficiently, and the cations are solvated by two bridging monodentate ligands, instead. However, K$^+$/tmeda chelates might still exist, e.g. in hexacoordinated ions.

D_{3h} carbon environment; the benzylsodium analogy. For $[CH_3A_2]^+$ model systems (A = Li, Na, or H), two isomers exist. For $[CH_5]^+$ (A = H), the covalent C_s structure with a cyclic three-centre-two-electron bond is preferred by (45.2 kJ mol^{-1}, MP4/6-311G**//6-31G*) [69] over the D_{3h} structure. In contrast, the D_{3h} geometry is preferred if A is Li or Na, i.e. an electropositive metal atom [69,70]. In order to minimize electrostatic interactions between the metal cations, they wish to be separated from each other as far as possible. However, the energetic preference for D_{3h} over C_s coordination is small (12.5–16.5 kJ mol^{-1} MP4/6-31G*//6-31G*, A = Na or Li). Hence, both structural types should be observable in organoalkali chemistry, with preference for local D_{3h} symmetry. In the crystal structure of benzylsodium · tmeda (**5**), two sodium cations coordinate with each of the benzylic CH_2 positions to give just this local D_{3h} geometry [38]. Indenylsodium · tmeda crystallizes in close analogy to **5**, with two sodium cations coordinating to the pseudo-benzylic position C(1) (local D_{3h} symmetry, angle NaC(7)Na′ 170.5°). Carbon–sodium bond distances are in the same range for both compounds (2.64 Å (**5**), and 2.58, 2.67 and 2.69 Å in **1**). The η^2-bridging of one of the sodium sites in **1** is paralleled by moderate bridging to the phenyl *ipso* carbon by two sodium sites in **5**. There seems to be but one major difference between both structures: **5** crystallizes as a tetrameric aggregate, whereas **1** forms infinite chains. However, this difference is not fundamental. For **5**, the angle NaC(7)Na′ angles are always oriented in the same direction of rotation, leading to the formation of cyclic tetramers. In **1**, these

angles possess alternate directions, leading to the formation of a puckered, planar chain. Thus **1** behaves as a benzyl, rather than as a cyclopentadienyl, derivative.

A structure quite analogous to that of **1** is found for benzyllithium · OEt_2 (**6**) [37]. The decrease in available coordination space from Na^+ to Li^+ is counterbalanced by a decrease to one solvation site. In the monomeric ion pair (dabco = 1,4-diazabicyclo[2.2.2]octane) structure of benzyllithium · dabco [71], additional solvation and increase in hapticity (η^3) counterbalances the loss of aggregation.

Experimental

Yellow crystals of **1** were synthesized by the addition of hexane-soluble [72] butylsodium · tmeda (2 cm^3; ca. 1 *M* solution) containing a threefold excess of tmeda to a petroleum ether solution (40 cm^3) of indene (1.5 mmol) at 0 °C, with the usual precautions for air-sensitive materials. After standing at −15 °C for one month, crystals of sufficient size had formed.

Acknowledgements

This work was supported by the Fonds der Chemischen Industrie and the Deutsche Forschungsgemeinschaft, and by the Fonds der Chemischen Industrie/Stiftung Volkswagenwerk with a Kekule-grant to C.S. We thank R.J. Bushby particularly for the electrostatic point charge calculations, helpful comments, and his interest in this work. E. Weiss and U. Schümann provided several results prior to publication, which we cordially acknowledge.

References

1 For a review of X-ray structures of organolithium compounds and a bibliography, see: W. Setzer and P.v.R. Schleyer, Adv. Organomet. Chem., 24 (1985) 353.
2 For a review of the structures of the higher organoalkali metal compounds and a bibliography, see: C. Schade and P.v.R. Schleyer, Adv. Organomet. Chem., 27 (1987) in press.
3 W.E. Rhine and G.D. Stucky, J. Am. Chem. Soc., 97 (1975) 737.
4 J.L. Atwood and K.D. Smith, J. Am. Chem. Soc., 96 (1974) 994.
5 T. Aoyagi, H.M.M. Shearer, K. Wade and G. Whitehead, J. Organomet. Chem., 175 (1979) 21.
6 R. Zerger, W. Rhine and G.D. Stucky, J. Am. Chem. Soc., 96 (1974) 5441.
7 (a) J.H. Burns and P.G. Laubereau, Inorg. Chem., 10 (1971) 2789;
(b) J.L. Atwood, W.E. Hunter, D.C. Hrncir, E. Samuel, H. Alt and M.D. Rausch, Inorg. Chem., 14 (1975) 1757;
(c) J.L. Atwood, J.H. Burns and P.G. Laubereau, J. Am. Chem. Soc., 95 (1973) 1830;
(d) M.E. Rerek and F. Basolo, J. Am. Chem. Soc., 106 (1984) 5908;
(e) R.T. Baker and T.H. Tulip, Organometallics, 5 (1986) 839;
(f) M.B. Honan, J.L. Atwood, I. Bernal and W.A. Herrmann, J. Organomet. Chem., 179 (1979) 403;
(g) A. Mawby and G.E. Pringle, J. Inorg. Nucl. Chem., 34 (1972) 525;
(h) F.S. Stephens, J. Chem. Soc., Dalton Trans., (1974) 13;
(i) P. Caddy, M. Green, E. O'Brien, L.E. Smart and P. Woodward, J. Chem. Soc., Dalton Trans., (1980) 962;
(j) S.R. Allen, P.K. Baker, S.G. Barnes, M. Bottrill, M. Green, A.G. Orpen, I.D. Williams and A.J. Welch, J. Chem. Soc., Dalton Trans., (1983) 927;
(k) Y.N. Al-Obaidi, M. Green, N.D. White, J.M. Barsett and A.J. Welch, J. Chem.Soc., Chem. Comm., (1981) 494;
(l) Y.N. Al-Obaidi, P.K. Baker, M. Green, N.D. White and G.E. Taylor, J. Chem. Soc., Dalton Trans., (1981) 2321;
(m) S.R. Allen, P.K. Baker, S.G. Barnes, M. Green, L. Trollope, L. Manojlovic-Muir and K.W. Muir, J. Chem. Soc., Dalton Trans., (1981) 873;

(n) J. Trotter, Acta Crystallogr., 11 (1958) 355;
(o) N.C. Webb and R.E. Marsh, ibid., 22 (1967) 382;
(p) Y.N. Al-Obaidi, M. Green, N.D. White and G.E. Taylor, J. Chem. Soc., Dalton Trans., (1981) 319;
(q) M. Green, J.C. Jeffrey, S.J. Porter, H. Razay and F.G.A. Stone, ibid., (1982) 2475;
(r) M. Green, J.A.K. Howard, S.J. Porter, F.G.A. Stone and D.C. Tyler, ibid., (1984) 2553;
(s) J.C. Jeffrey, C. Sambale, M.F. Schmidt and F.G.A. Stone, Organometallics, 1 (1982) 1597;
(t) J.W. Faller, R.H. Crabtree and A. Habib, ibid., 4 (1985) 929;
(u) P.M. Treichel, J.W. Johnson and J.C. Calabrese, J. Organomet. Chem., 88 (1975) 215;
(v) R. Shakir and J.L. Atwood, Acta Crystallogr., B, 37 (1981) 1656;
(w) G.G. Aleksandrov and Y.T. Struchkov, J. Strukt. Chem., 12 (1971) 99;
(x) P. Caddy, M. Green, E. O'Brien, L.E. Smart and P. Woodward, Angew. Chem., 89 (1977) 671; Int. Ed., Engl., 16 (1977) 648;
(y) D.E. Smith and A.J. Welch, Organometallics, 5 (1986) 760;
(z) W. Beeckman, J. Goffort, J. Rebizant and M.R. Spirlet, J. Organomet. Chem., 307 (1986) 23;
(aa) M. Mlekurz, P. Bougeard, B.G. Sayer, M.J. McGlinchey, A.C. Rodger, M. Rowen-Churchill, J.W. Ziller, S.K. Kang and T.A. Albright, Organometallics, 5 (1986) 1656;
(ab) K. Jonas, W. Rüssler, C. Krüger and E. Raabe, Angew. Chem., 98 (1986) 905; Int. Ed. Engl., 25 (1986) 928.
8 (a) A.N. Nesmeyanov, N.A. Ustynyuk, L.G. Makarova, V.G. Andrianov, Y.T. Struchkov, S. Andrae, Y.A. Ustynyuk and S.G. Malyugina, J. Organomet. Chem., 159 (1978) 189;
(b) R.M. Kowaleski, A.L. Rheingold, W.C. Trogler and F. Basolo, J. Am. Chem. Soc., 108 (1986) 2460;
(c) J.S. Merola, R.T. Kacmarcik and D. Van Engen, ibid., 108 (1986) 329.
9 J.M. O'Connor and C.P. Casey, Chem. Rev., 87 (1987) 307.
10 P. Main, S.E. Hull, L. Lessinger, G. Germain, J.P. Declerq and M.M. Woolfson, MULTAN 76, University of York, England, and Louvain, Belgium, 1976.
11 J.M. Stewart, P.A. Machin, C.W. Dickinson, H.L. Ammon, H. Heck and H. Flack, X-RAY 76, Technical Report TR 446, Computer Science Center, University of Maryland, 1976.
12 C.K. Johnson, ORTEP, Report ORNL-5138, Oak Ridge National Laboratory, Tennessee, 1976.
13 (a) J.B. Collins and S. Streitwieser, J. Comput. Chem., 1 (1980) 81;
(b) A.E. Reed, R.B. Weinstock and F. Weinhold, J. Chem. Phys., 83 (1985) 735;
(c) R.F.W. Bader and P.J. MacDougall, J. Am. Chem. Soc., 107 (1985) 6788.
14 E. Heilbronner and H. Bock, Das HMO-Modell und seine Anwendungen, Verlag Chemie, Weinheim, 1978.
15 (a) M.J.S. Dewar and W. Thiel, J. Am. Chem. Soc., 99 (1977) 4899, 4907;
(b) W. Thiel and T. Clark, to be published.
16 T. Clark, C. Rohde and P.v.R. Schleyer, Organometallics, 2 (1983) 1344.
17 R.H. Staley and J.L. Beauchamp, J. Am Chem. Soc., 97 (1975) 5920.
18 N. Trong Anh, M. Elian and R. Hoffmann, J. Am. Chem. Soc., 100 (1978) 110.
19 (a) P.v.R. Schleyer, Pure Appl. Chem., 55 (1983) 355; ibid., 56 (1984) 151;
(b) A. Streitwieser, Jr., Acc. Chem. Res., 17 (1984) 353;
(c) G. Boche, H. Etzrodt, W. Massa and G. Baum, Angew. Chem., 97 (1985) 858; Int. Ed. Engl., 24 (1985) 863.
20 (a) R.J. Bushby and M.P. Tytko, J. Organomet. Chem., 270 (1984) 265;
(b) R.J. Bushby, private communication.
21 (a) U. Edlund, Org. Magn. Res., 12 (1979) 661;
(b) C. Gooijer and N.H. Velthorst, Org. Magn. Res., 12 (1979) 684;
(c) M. Tsutsui and H.J. Gysling, J. Am. Chem. Soc., 91 (1969) 3175;
(d) J. van der Kooij, N.H. Velthorst and C. MacLean, Chem. Phys. Lett., 12 (1972) 596;
(e) J.B. Grutzner, J.M. Lawlor and L.M. Jackman, J. Am. Chem. Soc., 94 (1972) 2306;
(f) T. Schäfer and W.G. Schneider, Can. J. Chem., 41 (1963) 966;
(g) H.W. Vos, Y.W. Bakker, N.H. Velthorst and C. MacLean, Org. Magn. Res., 6 (1974) 574;
(h) J. van der Giessen, C. Gooijer, C. MacLean and N.H. Velthorst, Chem. Phys. Lett., 55 (1978) 33.
22 D.M. O'Brien, A.H. Hart and C.R. Russell, J. Am. Chem. Soc., 97 (1975) 4410.
23 A. Ceccon, A. Gambaro, A. Venzo, V. Lucchini, T.E. Bitterwolf and J. Shade, J. Organomet. Chem., 327 (1987) 55.

24 (a) M.F. Lappert, A. Singh, L.M. Engelhardt and A.H. White, J. Organomet. Chem., 262 (1984) 271;
(b) P. Jutzi, E. Schlüter, C. Krüger and S. Pohl, Angew. Chem., 95 (1983) 1015; Int. Ed. Engl., 22 (1983) 994;
(c) W.J. Evans, R. Dominguez, K.R. Levan and R.J. Doedens, Organometallics, 4 (1985) 1836;
(d) P. Jutzi, E. Schlüter, S. Pohl and W. Sack, Chem. Ber., 118 (1985) 1959.
25 E. Weiss, G. Sauermann and G. Thirase, Chem. Ber., 116 (1983) 74.
26 R.D. Rogers, J.L. Atwood, M.D. Rausch, D.W. Macomber and W.P. Hart, J. Organomet. Chem., 238 (1982) 79.
27 O. Mundt and G. Becker, Z. Anorg. Allg. Chem., 496 (1983) 58.
28 P. Jutzi, W. Leffers, B. Hampel, S. Pohl, and W. Saak, Angew. Chem., 99 (1987) 563; Int. Ed. Engl., 26 (1987) 584.
29 W. Binder and E. Weiss, J. Organomet. Chem., 92 (1975) 1.
30 H. Lehmkuhl, K. Mehler, R. Benn, A. Rufińska, and C. Krüger, Chem. Ber., 119 (1986) 1054.
31 (a) C.H. Wong, T.Y. Lee, T.J. Lee, T.W. Chang and C.S. Liu, Inorg. Nucl. Chem. Lett., 9 (1973) 667;
(b) K.W. Nugent, J.K. Beattie, T.W. Hambley and M.R. Snow, Aust. J. Chem., 37 (1984) 1601.
32 R. Zerger and G.D. Stucky, J. Organomet. Chem., 80 (1974) 7.
33 J.J. Brooks, W. Rhine and G.D. Stucky, J. Am. Chem. Soc., 94 (1972) 7346.
34 (a) U. Schümann, Dissertation, Hamburg, 1987;
(b) U. Schümann, E. Weiss, private communication.
35 J.J. Brooks, W. Rhine and G.D. Stucky, J. Am. Chem. Soc., 94 (1972) 7339.
36 For a recent example in lithium-thiolate chemistry, see: A.J. Banister, W. Clegg and W.R. Gill, J. Chem. Soc., Chem. Commun., (1987) 850.
37 M.A. Beno, H. Hope, M.M. Olmstead and P.P. Power, Organometallics, 4 (1985) 2117.
38 C. Schade, P.v.R. Schleyer, H. Dietrich and W. Mahdi, J. Am. Chem. Soc., 108 (1986) 2484.
39 E. Frasson, F. Menegus and C. Panattoni, Nature, 199 (1963) 1087.
40 J.F. Berar, G. Calvarin, C. Pommier and D. Weigel, J. Appl. Crystallogr., 8 (1975) 386.
41 C. Panattoni, G. Bombieri and U. Croatto, Acta Crystallogr., 21 (1966) 823.
42 H. Werner, H. Otto and H.J. Kraus, J. Organomet. Chem., 315 (1986) C57.
43 M.B. Freeman, L.G. Sneddon and J.C. Huffman, J. Am. Chem. Soc., 99 (1977) 5194.
44 (a) A. Haaland, S. Samdal and R. Seip, J. Organomet. Chem., 153 (1978) 178;
(b) T. Aoyagi, H.M.M. Shearer, M.M. Harrison, K. Wade and G. Whitehead, J. Organomet. Chem., 146 (1978) C29.
45 B. Tecle, P.W.R. Corfield and J.P. Oliver, Inorg. Chem., 21 (1982) 458.
46 J.L. Atwood and K.D. Smith, J. Am. Chem. Soc., 95 (1973) 1488.
47 S.H. Eggers, J. Kopf and R.D. Fischer, Organometallics, 5 (1986) 383.
48 W. Bünder and E. Weiss, Z. Naturforsch. B, 33 (1978) 1235.
49 (a) W. Siebert, Angew. Chem., 97 (1985) 924; Int. Ed. Engl.;
(b) T. Kuhlmann, S. Roth, J. Rozière and W. Siebert, ibid., 98 (1986) 87; Int. Ed. Engl., 25 (1986) 105.
50 (a) F.A. Cotton, A. Musco and G. Yagupsky, J. Am. Chem. Soc., 89 (1967) 6136;
(b) F.A. Cotton and T.J. Marks, J. Am. Chem. Soc., 91 (1969) 3178;
(c) C.P. Casey and J.M. O'Connor, Organometallics, 4 (1985) 384.
51 H. Köster and E. Weiss, Chem. Ber., 115 (1982) 3422.
52 U. Schühmann, E. Weiss, H. Dietrich and W. Mahdi, J. Organomet. Chem., 322 (1987) 299.
53 G. Boche, H. Etzrodt, M. Marsch, W. Massa, G. Baum, H. Dietrich and W. Mahdi, Angew. Chem., 98 (1986) 84; Int. Ed. Engl., 25 (1986) 104.
54 (a) F.H. Köler, Chem. Ber., 107 (1974) 570;
(b) M.L.H. Green, N.D. Lowe and D. O'Hare, J. Chem. Soc., Chem. Commun., (1986) 1547.
55 (a) A.J. Hart-Davis and R.J. Mawby, J. Chem. Soc. A, (1969) 2403;
(b) C. White, R.J. Mawby and A.J. Hart-Davis, Inorg. Chim. Acta, 4 (1970) 441;
(c) M.E. Rerek and F. Basolo, J. Am. Chem. Soc., 106 (1984) 5908;
(d) M.E. Rerek, L.-N. Ji and F. Basolo, J. Chem. Soc., Chem. Commun., (1983) 1208.
56 P. Jutzi, Chem. Rev., 87 (1987) 983.
57 E. Kaufmann and P.v.R. Schleyer, unpublished calculations.
58 H. Dietrich, W. Mahdi, D. Wilhelm, T. Clark and P.v.R. Schleyer, Angew. Chem., 96 (1984) 623; Angew. Chem. Int. Ed. Engl., 23 (1984) 621.
59 D. Wilhelm, H. Dietrich, W. Mahdi and P.v.R. Schleyer, unpublished results.

60 G. Boche, G. Decker, H. Etzrodt, H. Dietrich, W. Mahdi, A. Kos and P.v.R. Schleyer, J. Chem. Soc., Chem. Commun., (1984) 1493.
61 D. Wilhelm, T. Clark, P.v.R. Schleyer, H. Dietrich and W. Mahdi, J. Organomet. Chem., 280 (1985) C6.
62 W. Neugebauer, P.v.R. Schleyer, H. Dietrich and W. Mahdi, unpublished results.
63 D. Thoennes and E. Weiss, Chem. Ber., 111 (1978) 3157.
64 J.J. Brooks and G.D. Stucky, J. Am. Chem. Soc., 94 (1972) 7333.
65 M. Walczak and G.D. Stucky, J. Am. Chem. Soc., 98 (1976) 5531.
66 H. Köster and E. Weiss, J. Organomet. Chem., 168 (1979) 273.
67 C. Schade, P.v.R. Schleyer, M. Geisler, and E. Weiss, Angew. Chem., 98 (1986) 922; Int. Ed. Engl., 25 (1986) 902.
68 (a) K.R. Pörschke, W. Kleinmann, G. Wilke, K.H. Claus, C. Krüger, Angew. Chem., 95 (1983) 1032; Int. Ed. Engl., 22 (1983) 991;
(b) R. Goddard, C. Krüger, K.R. Pörschke and G. Wilke, J. Organomet. Chem., 308 (1986) 85.
69 K. Raghavachari, R.A. Whiteside, J.A. Pople and P.v.R. Schleyer, J. Am. Chem. Soc., 103 (1981) 5649.
70 (a) E.D. Jemmis, J. Chandrasekhar and P.v.R. Schleyer, J. Am. Chem. Soc., 101 (1979) 527;
(b) E.D. Jemmis, J. Chandrasekhar, E.-U. Würthwein, P.v.R. Schleyer, B. Chinn and J.A. Pople, J. Am. Chem. Soc., 104 (1982) 4275;
(c) P.v.R. Schleyer, P. Tidor, E.D. Jemmis, J. Chandrasekhar, E.-U. Würthwein, A.J. Kos, B.T. Luke and J.A. Pople, J. Am. Chem. Soc., 105 (1983) 484.
71 S.D. Patterman, I.L. Karle and G.D. Stucky, J. Am. Chem. Soc., 92 (1970) 1150.
72 C. Schade, W. Bauer and P.v.R. Schleyer, J. Organomet. Chem., 295 (1985) C25.